63-2-5

PHILCO CORPORATION — Western Development Laboratories

In reply cite: 614-3-178
RWB/EHG:pjc
27 February 1963

SUBJECT: Contract AF04(695)-113
Submission of Technical Report WDL-TR2035
As a deliverable item

TO: Commander
Space Systems Division
Air Force Systems Command
United States Air Force
Air Force Unit Post Office
Los Angeles 45, California

ATTENTION: Technical Data Center

INFO COPIES: D. Cowart, CSD #3 (1 copy)
B. Byrd, AFSSD/SSOCK (w/o enclosure)
ASTIA, Arlington, Va. (2 copies)

REFERENCE: (a) Contract AF04(695)-113, Exhibit "A"
(b) Section IV, Paragraph 4.2.2 of AFBM Exhibit 58-1
(c) Paragraph 1.2.1.2 of AFSSD Exhibit 61-27A

In accordance with the requirements of references (a), (b), and (c), we are forwarding ten (10) copies of the following document:

Title	No. and Date
FGS Antenna Resonance Study	WDL-TR2035 27 February 1963

PHILCO CORPORATION
Western Development Laboratories

R. W. Boyd

R. W. Boyd
Manager, Contracts Management

WDL-TR2035

TECHNICAL DOCUMENTARY REPORT

27 FEBRUARY 1963

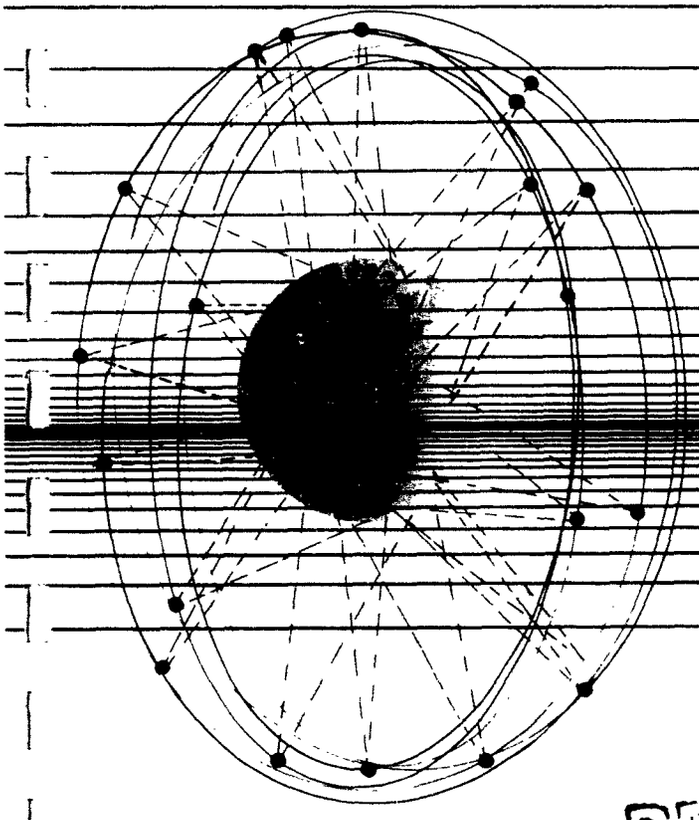

FGS ANTENNA RESONANCE STUDY

by HUGH L. SMITH
and HENRY B. LEE

PREPARED FOR:

AIR FORCE SPACE SYSTEMS DIVISION
AIR FORCE SYSTEMS COMMAND
UNITED STATES AIR FORCE
INGLEWOOD, CALIFORNIA

CONTRACT NO. AF04(695)-113

PHILCO
A SUBSIDIARY OF Ford Motor Company

WESTERN DEVELOPMENT LABORATORIES
PALO ALTO, CALIFORNIA

WDL-TR2035
27 February 1963

TECHNICAL DOCUMENTARY REPORT

FGS ANTENNA RESONANCE STUDY

by

Hugh L. Smith and Henry B. Lee

Prepared by

PHILCO CORPORATION
Western Development Laboratories
Palo Alto, California

Contract AF04(695)-113

Prepared for

SPACE SYSTEMS DIVISION
AIR FORCE SYSTEMS COMMAND
UNITED STATES AIR FORCE
Inglewood, California

SUMMARY

This report contains the results which were obtained from two series of tests and an analytical investigation conducted to determine the mechanical dynamic characteristics of the three-axis T&D antenna system at FGS.

Section 1 contains introductory material and general comments which relate to antenna design, test, and analysis.

In Section 2, the method of analysis is given with differential equations of motion which describe the system. The analysis of individual components which make up the mathematical model is discussed.

The results of the theoretical analysis are given in Section 3 in the form of structural transfer functions which yield outputs of coordinates on the antenna. Transfer functions are interpreted to yield the natural frequencies and the locked-rotor frequencies of the antenna.

The field test results are presented in Section 4, together with a discussion of the correlation between these test values and the analytical results.

Section 5 contains a discussion of the areas which govern antenna behavior, together with some suggested modifications which will upgrade antenna performance.

ABSTRACT

PHILCO WDL-TR2035 UNCLASSIFIED

FGS ANTENNA RESONANCE STUDY

by Hugh L. Smith and
Henry B. Lee 41 pages

27 February 1963 Contract No. AF04(695)-113

This report contains the results which were obtained from two series of tests and an analytical investigation conducted to determine the mechanical dynamic characteristics of the three-axis T&D antenna system at FGS.

Subjects which are discussed are method of analysis, results of the theoretical analysis, field test results, a discussion of the areas which govern antenna behavior, and suggested modifications which will upgrade antenna performance.

THIS UNCLASSIFIED ABSTRACT IS DESIGNED FOR RETENTION IN A STANDARD 3-BY-5 CARD-SIZE FILE, IF DESIRED. WHERE THE ABSTRACT COVERS MORE THAN ONE SIDE OF THE CARD, THE ENTIRE RECTANGLE MAY BE CUT OUT AND FOLDED AT THE DOTTED CENTER LINE. (IF THE ABSTRACT IS CLASSIFIED, HOWEVER, IT MUST NOT BE REMOVED FROM THE DOCUMENT IN WHICH IT IS INCLUDED.)

FOREWORD

This Technical Documentary Report on Definitive Contract AF04(695)-113 has been prepared in accordance with Exhibit "A" of that contract and Paragraph 4.2.2 of AFBM of AFBM Exhibit 58-1, "Contractor Reports Exhibit," dated 1 October 1959, as revised and amended.

This report was prepared by Philco Western Development Laboratories in fulfilling the requirements of Paragraph 1.2.1.2 of AFSSD Exhibit 61-27A, "Satellite Control Subsystem Work Statement," dated 15 February 1962, as revised and amended.

TABLE OF CONTENTS

LIST OF ILLUSTRATIONS

SECTION 1

INTRODUCTION

1.1 GENERAL

During 1962, two series of tests were conducted to determine the mechanical dynamic characteristics of the three-axis T&D antenna system at FGS. (See Fig. 1-1.) The second series was run because subsequent WDL experience in dynamic analysis and testing of large antennas indicated that a more comprehensive definition of these characteristics could be obtained by the use of more sophisticated instrumentation and test procedures. Also, the additional data obtained was necessary in order to determine the validity of various techniques used to determine analytically the dynamic characteristics of large antenna structures.

Knowledge of the dynamic characteristics of the antenna structure is necessary in designing a control system for specified performance. This information is needed to determine motive power requirements and the dynamic response of points in the system at which feedback sensors are mounted. In small systems in which the controlled loads have high resonant frequecies, elastic distortions of the load may be relatively unimportant, but in large systems, such as antenna systems, the stuctural deformations due to dynamic loads may significantly affect over-all system performance.

In a system with rate (tachometer) feedback, for example, the closed loop bandwidth is limited by the lowest locked-rotor frequency.* Auto-Tracking capability is limited by the mechanical natural frequency of the feed support system.

---

* Locked-rotor frequency is the natural frequency of the antenna when the motor drive shaft is fixed relative to the antenna (brakes locked). At this frequency, there is a severe dip in the tachometer frequency response function.

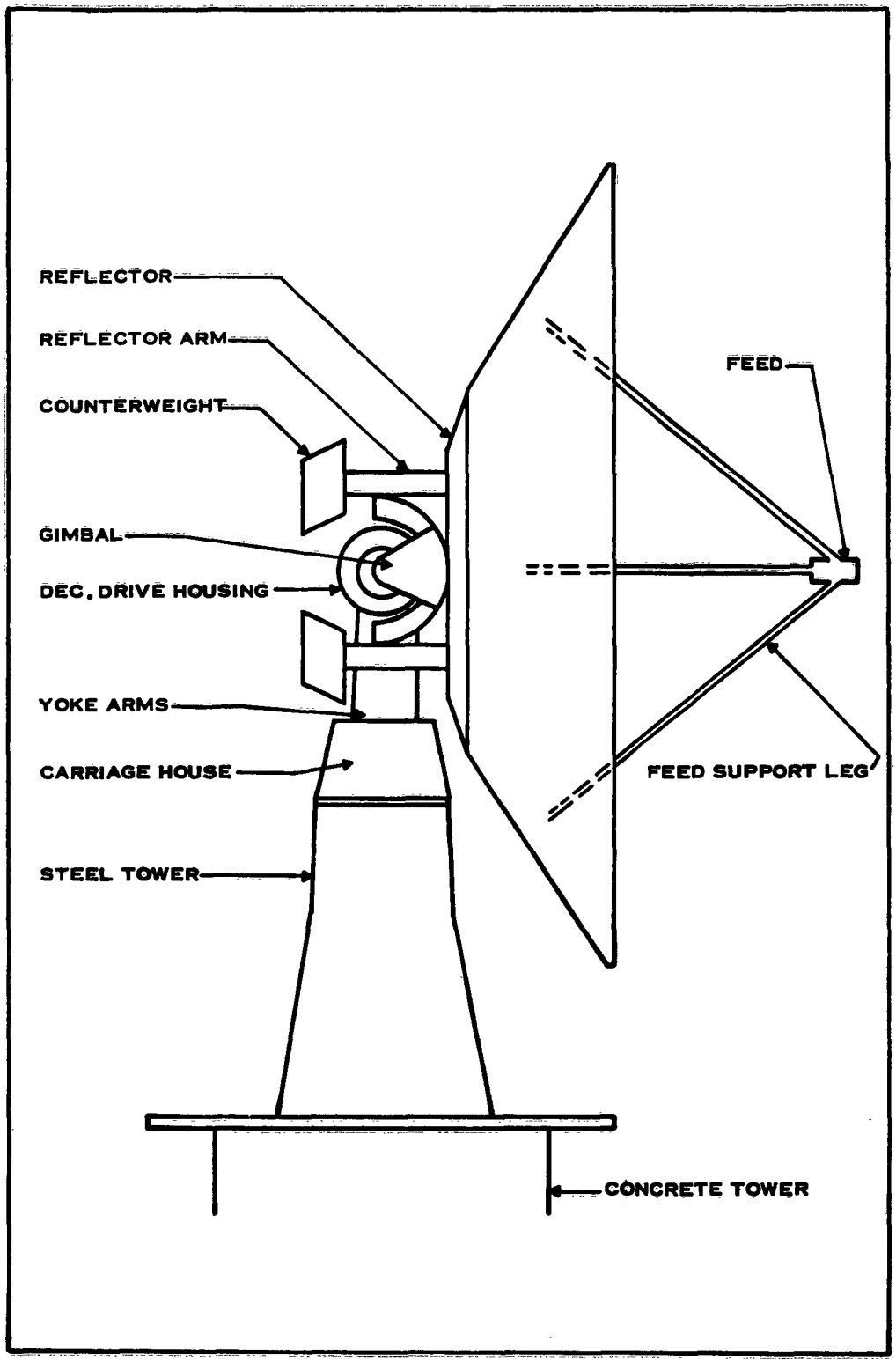

FIG. I-I ANTENNA NOMENCLATURE

Because of the effects of structural dynamics on over-all system performance, it is desirable to be able to predict these characteristics during the design phase in order to assure that performance specifications will be met, and, in the case of an already completed system, it is desirable to be able to determine analytically which elements of a system should be modified to upgrade performance if desired. The requisite analytical capability can be acquired only by carrying out a series of analyses and tests of particular structures and by comparing the results of both.

Experience with the FGS T&D antenna yielded comprehensive field data, and provided WDL with an ideal opportunity to develop and test analytical techniques which were developed during the past year in their Antenna Systems Laboratory. In addition, WDL, through its experience, determined problem areas in the FGS antenna structure.

Because of the rigorous time schedule of this project, the antenna was analyzed in only one orientation. The response of the structure to azimuth driving with the antenna looking at the horizon was calculated, because the tracking rate and acceleration requirements are considerably more severe on the azimuth axis than on the elevation axis. The lowest azimuth locked-rotor frequency was measured with the antenna on horizon. In this orientation, analysis of a particularly complex model was required. The complexity of this model permitted investigation of phenomena such as coupled vibration modes.

The model analyzed has 25 degrees of freedom, including translational and rotational displacements. An undamped forced-vibration analysis was performed, with the system being driven by the servo drive system as it is in actual operation. Transfer functions were calculated for the response of various points in the system; during the field tests, displacements were measured at these points. The poles and zeros

of these transfer functions give various characteristic frequencies of the system, and can be correlated with fluctuations in the measured frequency response functions.

Individual components, and combinations of components were analyzed to determine the cause of the low measured frequencies. These analyses are described in Section 5 of this report.

An identical analysis of the IOS antenna system was conducted concurrently with the FGS analysis. Since both antennas have the same pedestal and drive system, only the moving antenna structure required a different model from that of FGS. Because the IOS antenna has no third axis, and because its structural attachment of the reflector to the elevation axis is considerably stiffer than its counterpart on the FGS antenna, the lowest locked-rotor frequency is considerably higher than the lowest FGS locked-rotor frequency.

Upon completion of the FGS study, additional analysis will be performed to determine structural transfer functions of the IOS antenna in other orientations.

1.2 SCOPE

In Section 2, the method of analysis is given with differential equations of motion which describe the system. The analysis of individual components which make up the mathematical model is discussed.

The results of the theoretical analysis are given in Section 3 in the form of structural transfer functions which yield outputs of coordinates on the antenna. Transfer functions are interpreted to yield the natural frequencies and the locked-rotor frequencies of the antenna.

The field test results are presented in Section 4, together with a discussion of the correlation between these test values and the analytical results.

Section 5 contains a discussion of the areas which govern antenna behavior, together with some suggested modifications which will upgrade antenna performance.

SECTION 2

DYNAMIC ANALYSIS

2.1 ANALYTICAL METHOD

The dynamic characteristics of the antenna structure are determined by analyzing it as a lumped-mass model. The locations at which inertia is assumed to be concentrated are determined by application of engineering judgement to the specific structural design configuration. For example, components which might be expected to move together more or less as a rigid body are considered to be concentrated together. Another consideration is that the total number of lumps necessary for a given model obviously must be greater than the number of modes of vibration to be described by the model.

When the locations of the inertia lumps are determined, the mass and moment of inertia to be concentrated at each location are calculated from design drawings. Then the flexibility of elements connecting the various lumps is calculated by various structural analysis techniques, including digital computer truss and frame analyses. These elastic coefficients are expressed as matrices of influence coefficients.

When these mechanical parameters of the structure have been so determined, equations of motion describing the response of the system to a driving torque are formulated. These equations involve the inertia and elasticity of the lumped elements of the structure and the kinematics of the system, and include such factors as the flexibility of the gear train and bearings. These equations of motion are a system of linear differential equations in the various displacements and rotations of the lumped inertia elements which describe the state of the system, and various other quantities of interest, such as r-f beam position, rotation of drive-motor shaft, motion of control system sensors, etc.

This analysis is essentially a forced, rather than a free, vibration analysis. This approach is used because, in overall system design

and analysis, the required information is a knowledge of the dynamic response of the structure. The antenna structure acts as the load on the drive system, and complete system response characteristics depend on load characteristics. Also, vital parameters, such as the motion of the r-f beam, are controlled by the motions of the structure.

Transfer functions describing the motion of various points in the system can be determined from this system of equations. The poles and zeros of these transfer functions are calculated by means of a computer program which determines the characteristic roots of a determinant whose elements are quadratic functions of the Laplace operator s. Another available computer program, which computes system influence coefficients from local elastic parameters and lowest natural frequency and mode shape for simple structures, is used to determine many of the parameters used in the above system of equations, and to determine from simplified models of the system the cause of various system resonances.

Special techniques which are used to compute compliance, and other dynamic parameters, of certain components are described in Para. 2.3.

2.2 MATHEMATICAL MODEL AND EQUATIONS OF MOTION

A lumped mass-spring model was used in the dynamic analysis of the antenna structure. The antenna and the corresponding lumped-mass model with the forces acting on it are shown in Fig. 2-1. Because D'Alembert's method was used, inertia forces are shown. The model used has 25 degrees of freedom. The complexity of this model was necessary for the following reasons:

a. In the orientation analyzed, lateral motion of the pedestal is inherently coupled with rotation of the antenna about the vertical axis.

b. The moving structure is elastically unsymmetric about the reflector axis.

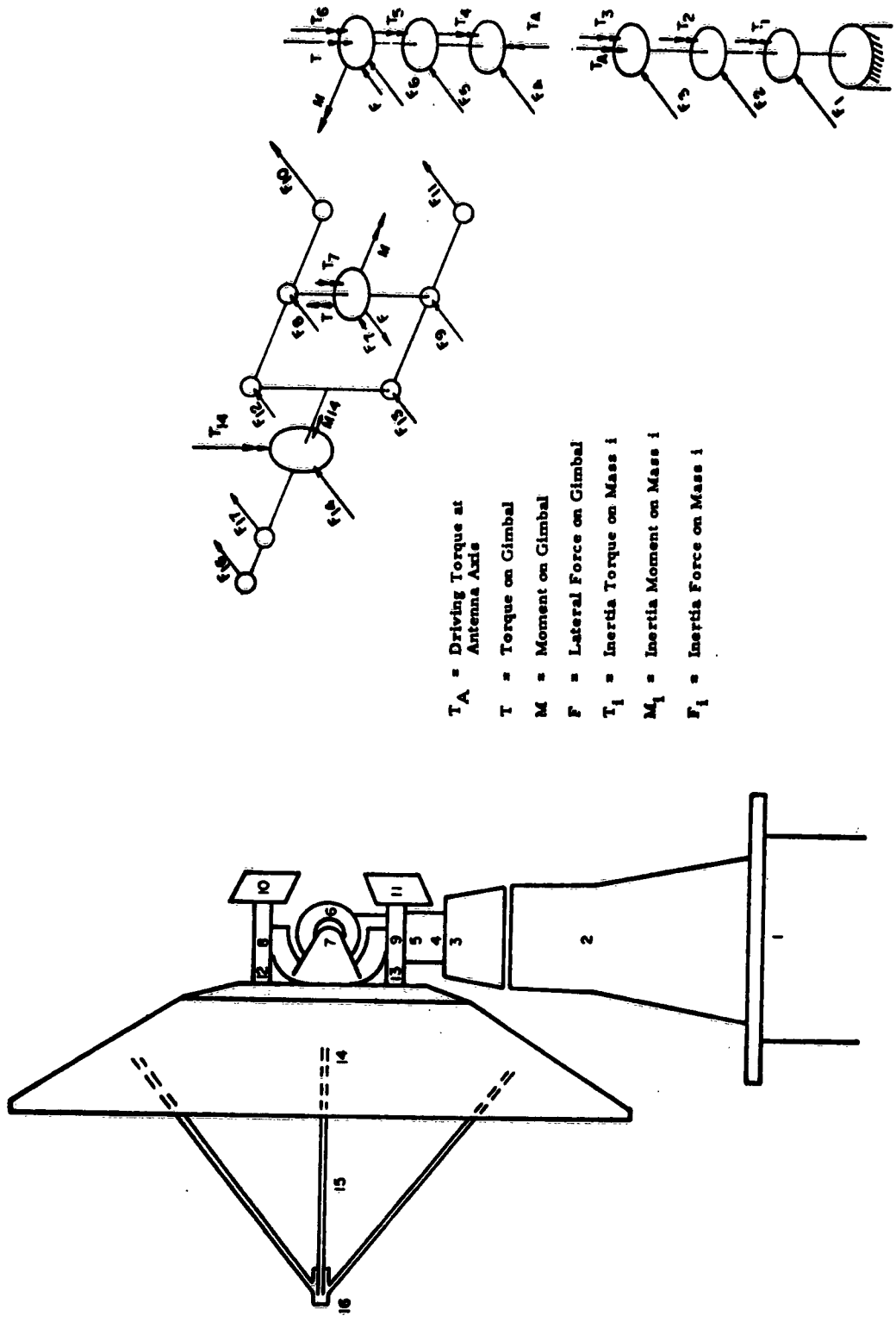

Fig. 2-1 View of Antenna Showing Locations of Mass Lumps and Free Body Diagrams Showing Forces Acting on Lumped Mass Model

c. In order to define several modes of vibration of a continuous structure, it is necessary to have several lumps per mode required. (A rough rule of thumb is that four to six lumps are required per mode determined.)

The complexity of this model should thus make it possible to calculate several of the higher modes observed in the field tests. No damping was included in the model, since it is known that structural damping is small and only slightly affects the significant frequencies; also, damping would complicate the analytical problem considerably. The static balance and total moment of inertia of the model were compared with corresponding parameters for the actual antenna as a check on the mass lumping.

Representative examples of the system of simultaneous equations of motion are given. In these equations, x is a lateral displacement coordinate, and θ and ϕ are, respectively, rotations about the azimuth and reflector axes. Operational notation is used where the operator s may be thought of as the differential operator $\frac{d}{dt}$ or as a Laplacian operator.

$$X_i = - \sum_{j=1}^{6} \delta_i^{Fj} m_j s^2 x_j - \delta_i^{F6} F - \delta_i^{M6} M \qquad (2\text{-}1)$$

$$\theta_i = - \sum_{j=1}^{3} \theta_i^{Tj} I_j s^2 \theta_j - \theta_i^{T6} T_A \qquad (2\text{-}2)$$

$$F = \sum_{i=7}^{16} m_i s^2 x_i \qquad (2\text{-}3)$$

$$T = \sum_{10}^{16} z_i m_i s^2 x_i + \sum_{i=7}^{14} I_i s^2 \theta_i \qquad (2\text{-}4)$$

$$\theta_i - \theta_4 = -\sum_{j=5}^{6} \theta_i^{Tj} I_j s^2 \theta_j - \theta_i^{T6} T \qquad (2\text{-}5)$$

$$\phi_{14} - \phi_7 = -\sum_{j=8}^{16} \phi_{14}^{Fj} m_j s^2 x_j - \phi_{14}^{M14} J_{14} s^2 \phi_{14}$$

$$- \phi_{14}^{T14} I_{14} s^2 \theta_{14} \qquad (2\text{-}6)$$

x_i = Coordinate of cg of lump i measured positively along the reflector axis from the declination axis.

m_i = Mass of lump i.

I_i = Moment of inertia of lump i about a vertical axis.

J_i = Moment of inertia of lump i about the reflector axis.

δ_i^{Fj} = Displacement of lump i due to the application of unit lateral force to lump j.

δ_i^{Mj} = Displacement of lump i due to the application of a unit moment about a horizontal axis at lump j.

δ_i^{Tj} = Displacement of lump i due to the application of a unit moment about a vertical axis at lump j.

Influence coefficients for rotations use the same subscript and superscript conventions as the above with δ being replaced by θ for rotation about a vertical axis and by ϕ for rotation about a horizontal axis parallel to the reflector axis.

These equations are solved to yield transfer functions for the response of various points in the system to the applied driving torque. The poles of these transfer functions are pure imaginary because the system is undamped and they correspond to system resonant frequencies. This transfer function representation corresponds to reducing the system of simultaneous differential equations to another set of simultaneous equations in which each of which only one of the dependent variables appears.

The results of this analysis are discussed in Section 3.

2.3 COMPONENT FLEXIBILITY ANALYSIS

The dynamic analysis, as delineated in Para. 2.2, required that the elastic behavior of the system be determined. This was accomplished by evaluating the elastic deformations of each component and by combining these elements to obtain the compliance parameters to be used as coefficients in the differential equations.

2.3.1 Structural Analysis

Rotation and displacement coefficients were calculated for all elements due to forces and moments at every element. These coefficients, arranged in the proper array, make up the flexibility coefficient matrix. The methods used to determine these coefficients were those of ordinary structural analysis, such as the Virtual Work Method or the Conjugate Beam Method. For the more complex parts of the structure, a digital computer program for analysis of three-dimensional framed structures was used to determine the influence coefficients. For example, all the structure beyond the gimbal (i.e., the reflector, reflector arms, counterweights, and equivalent feed system) was analyzed as a unit, using this computer program.

The side elevation of that structure, together with the representative mathematical model, is shown in Fig. 2-2. This model includes the flexibilities of the transverse shafts and bearings and

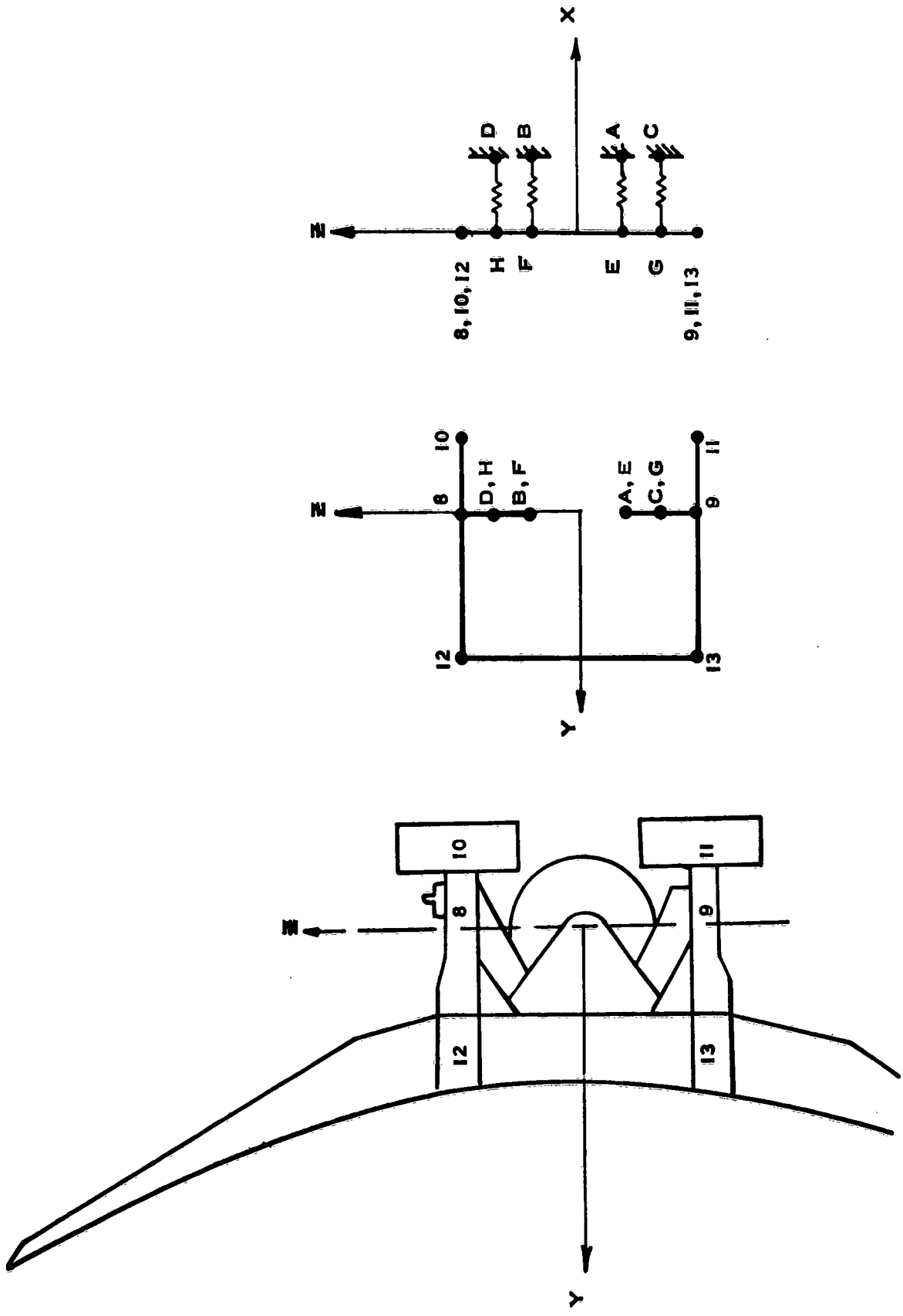

Fig. 2-2 Mathematical Model of Reflector, Reflector Arms, and Counterweights

transverse gearboxes on the upper reflector arm (lower arm is ungeared). Because of the asymmetry and the degree of indeterminancy of the structure, the frame analysis computer program was used to advantage here as it was in other areas of the antenna.

2.3.2 Feed System Analysis

A rather complete static and dynamic analysis was made of the feed system (composed of the feed and the feed support legs). A nine-degree-of-freedom lumped parameter model was used (see Fig. 2-3). The feed support legs were represented by an equivalent mass located at the center of mass of the leg; the feed itself was represented by a rotary inertia only, because the translation of the mass at the feed support.

The motion of each feed leg lump was described by two orthogonal displacements normal to the leg, and the motion of the feed was described by a rotation about the reflector axis. Finally, the dynamic behavior of the system was described by a set of ordinary differential equations, the solution of which yields the natural frequencies of the feed system. These frequencies fell mostly in the two ranges of 4.4-5.0 cps and 7.0-8.0 cps.

These analytical results bracket the feed system resonant frequencies of 4.6, 5.0, 7.1, and 7.5 cps, which were observed during the FGS Vibration Tests, Series I. Past studies of structural transfer functions have shown that the natural frequencies of the feed system are not reflected throughout the antenna structure simply because the mass of the feed system is small compared to that of the rest of the structure. For this reason, it was not necessary to use such a complex model in the overall mathematical model of the antenna. A simplified model with parameters which yielded a 5 cps resonant frequency was used. Again it must be emphasized that this was justified, because the dynamic response characteristics of the feed system were completely known, and because the forces generated by the feed system during resonance do not appreciably affect the other structural components.

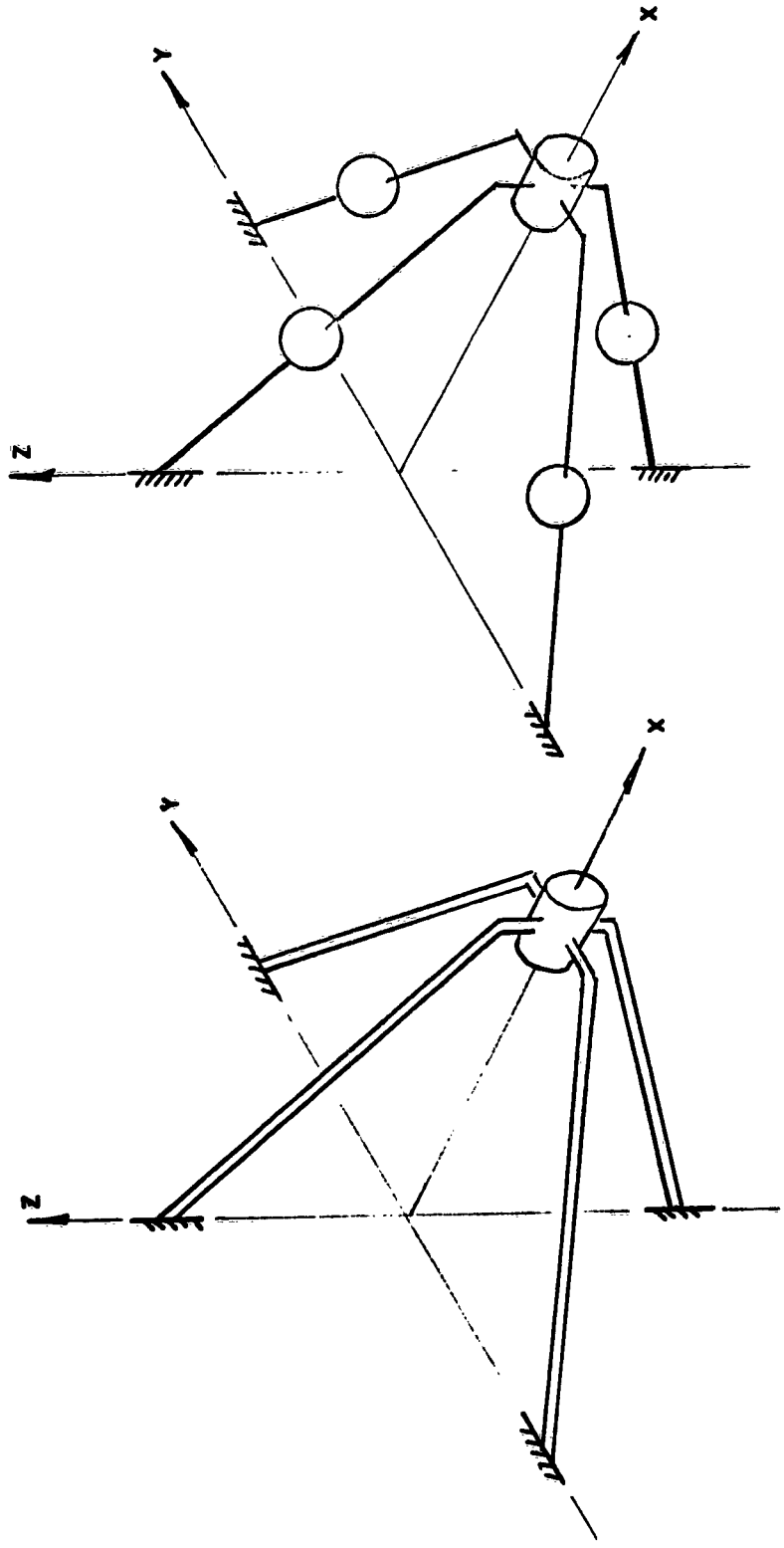

Fig. 2-3 Nine Degrees-of-Freedom Mathematical Model of Feed and Feed Support Structure

2.3.3 Bearings

The bearings which support the declination and transverse axes were among the more flexible links in the antenna structure. For example, the gimbal coefficients increased by a factor of five when the bearings were included. This problem was recognized earlier, and full size tests were conducted in which the deflections of the pinion shaft bearings were physically measured on an antenna simulator at WDL. These measurements do not compare exactly with those obtained by theoretical computation. Although the test and calculated values were of the same magnitude, they differed by a factor of as much as two. The method used to determine bearing stiffness was that presented by Palmgren* and will not be described in detail here.

In general, the literature on bearings does not treat the problem of deflections, and methods of computations which are available give only approximate values.

2.3.4 Gearboxes

Gearbox flexibility was obtained from bench tests performed by the manufacturer. In this type of test, the pinion shaft is fixed at the spline, and the rotation of the input shaft is measured for a known applied torque. This test does not accurately predict the flexibility of the gearbox as mounted on the antenna, since it does not include deformations other than those which occur in the gearbox itself. Previous tests of a similar gearbox mounted on an antenna simulator and previous theoretical calculations made at WDL have accounted for additional elastic deformations, such as those of the gear teeth, the pinion shaft with bearings, and gearbox mounting structure. Analysis and testing both showed that the compliance obtained was approximately 50 percent greater than that which was due to wind-up in the gearbox shafts; because of this experience, the manufacturer's value was increased accordingly.

---

* Palmgren, A., Ball and Roller Bearing Engineering, SKF Industries Inc., Phila., Pa., 1945.

SECTION 3

RESULTS OF ANALYSIS OF EXISTING STRUCTURE

The system of differential equations of motion in Section 2 can be reduced to yield transfer functions which describe displacements, velocities and accelerations of particular components of interest on the antenna. The transfer function is a ratio of output to input of a dynamical system expressed in operational form and is commonly expressed as the function of complex operator s.

The following transfer functions are given for outputs of motor-shaft rotation, reflector translation, reflector rotation about its own axis, and translation of the tower at the azimuth bearing for an azimuth motor torque input with the reflector horizon oriented. Coordinates for which transfer functions were calculated are shown in Fig. 3-1.

Transfer Functions

$$\frac{\theta_M}{T_M} = \frac{\left(1+\frac{s^2}{(2\pi 2.66)^2}\right)\left(1+\frac{s^2}{(2\pi 3.78)^2}\right)\left(1+\frac{s^2}{(2\pi 5.00)^2}\right)\left(1+\frac{s^2}{(2\pi 6.06)^2}\right)\left(1+\frac{s^2}{(2\pi 12.3)^2}\right)}{1047s^2\left(1+\frac{s^2}{(2\pi 3.47)^2}\right)\left(1+\frac{s^2}{(2\pi 4.11)^2}\right)\left(1+\frac{s^2}{(2\pi 5.02)^2}\right)\left(1+\frac{s^2}{(2\pi 9.87)^2}\right)\left(1+\frac{s^2}{(2\pi 16.1)^2}\right)}$$

$$\frac{X_R}{T_M} = \frac{\left(1+\frac{s^2}{(2\pi 3.33)^2}\right)\left(1+\frac{s^2}{462}+\frac{s^4}{921^2}\right)\left(1+\frac{s^2}{(2\pi 11.0)^2}\right)\left(1+\frac{s^2}{(2\pi 19.54)^2}\right)}{16080s^2\left(1+\frac{s^2}{(2\pi 3.47)^2}\right)\left(1+\frac{s^2}{(2\pi 4.11)^2}\right)\left(1+\frac{s^2}{(2\pi 5.02)^2}\right)\left(1+\frac{s^2}{(2\pi 9.87)^2}\right)\left(1+\frac{s^2}{(2\pi 16.1)^2}\right)}$$

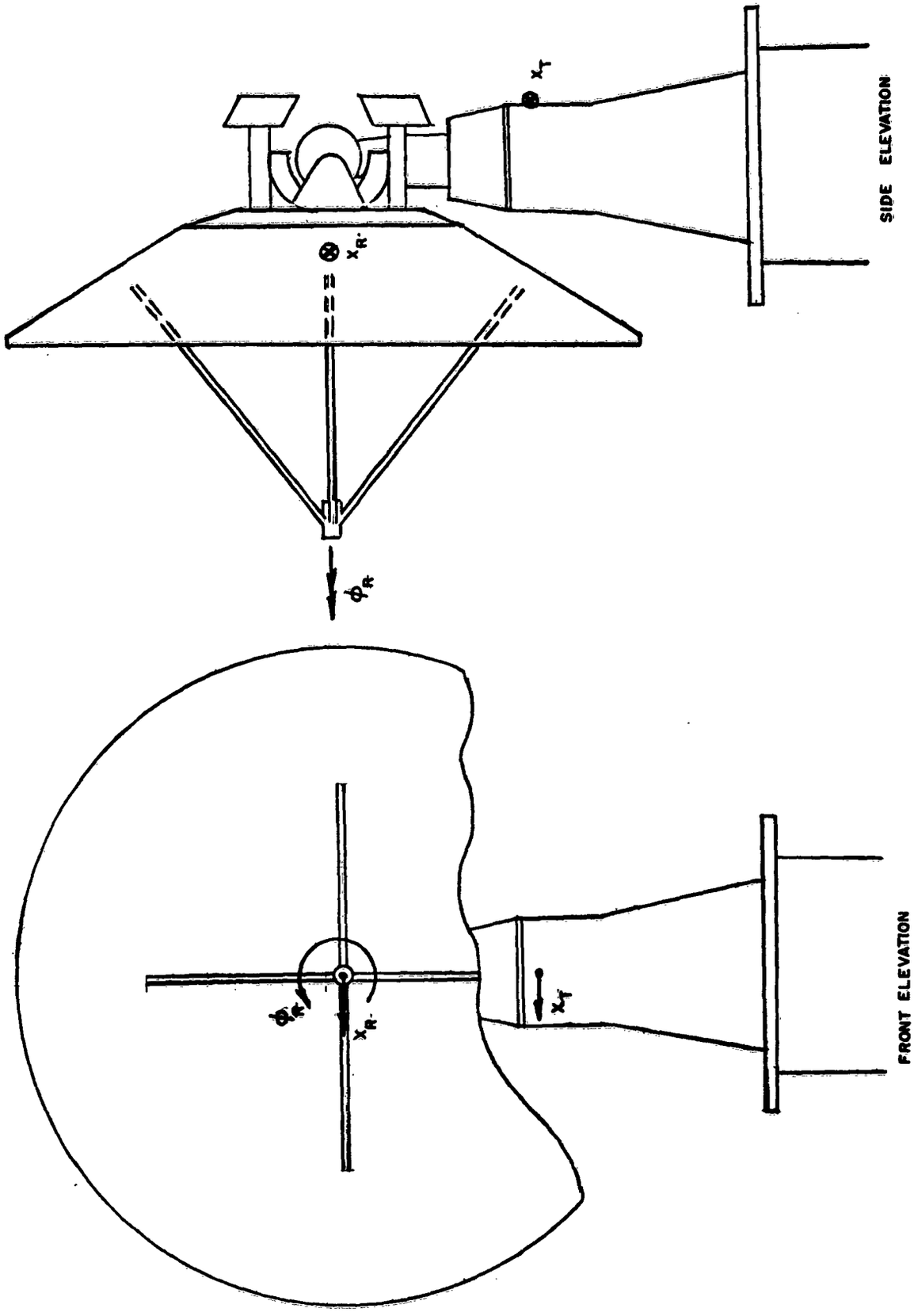

Fig. 3-1 Displacements for which Frequency Response Functions are Determined

$$\frac{\phi_R}{T_M} = \frac{\left(1+\frac{s^2}{(2\pi 3.84)^2}\right)\left(1+\frac{s^2}{(2\pi 5.03)^2}\right)\left(1+\frac{s^2}{(2\pi 12.7)^2}\right)\left(1+\frac{s^2}{(2\pi 20.4)^2}\right)}{15.5\left(1+\frac{s^2}{(2\pi 3.47)^2}\right)\left(1+\frac{s^2}{(2\pi 4.11)^2}\right)\left(1+\frac{s^2}{(2\pi 5.02)^2}\right)\left(1+\frac{s^2}{(2\pi 9.87)^2}\right)\left(1+\frac{s^2}{(2\pi 16.1)^2}\right)}$$

$$\frac{X_T}{T_M} = \frac{\left(1-\frac{s^2}{10.17^2}\right)\left(1+\frac{s^2}{(2\pi 5.07)^2}\right)\left(1-\frac{s^2}{45.56^2}\right)}{33.2\text{X}10^8\left(1+\frac{s^2}{(2\pi 3.47)^2}\right)\left(1+\frac{s^2}{(2\pi 4.11)^2}\right)\left(1+\frac{s^2}{(2\pi 5.02)^2}\right)\left(1+\frac{s^2}{(2\pi 9.87)^2}\right)\left(1+\frac{s^2}{(2\pi 16.1)^2}\right)}$$

where

X_R = transverse translation of the reflector

X_T = transverse translation of the tower

θ_M = rotation of the motorshaft

ϕ_R = rotation of the reflector about its axis of symmetry

T_M = azimuth motor torque

Not all of the factors of the numerators and denominators of the above transfer are given because the primary interest is in the low frequency response of antenna structures. Also, the higher modal frequencies of a continuous structure cannot be accurately calculated using a lumped parameter model.

The poles of these transfer functions physically represent the natural frequencies of the antenna with zero input torque (free at the azimuth axis). At frequencies corresponding to these poles, peaks appear on the frequency response curves because the amplitudes are

highly magnified at these system resonant frequencies. When there is a transfer function zero at a frequency close to a system resonant frequency, the cancelling effect of such a pole-zero dipole attenuates the amplitude variation of both the pole and the zero in a realistic, undamped system, sometimes making their presence imperceptible.

The zeros of the transfer function represent the frequencies at which zero response occurs and are manifested in dips in the frequency response curves. In the case of the motorshaft rotation transfer function, the zeros represent the locked-rotor frequencies which are the natural frequencies of the antenna structure when the motorshaft is constrained from rotation relative to the antenna. The lowest locked-rotor frequency calculated was 2.6 cps. This frequency is significant in that it is where the control system senses an amplitude attenuation and phase shift when it observes the response of the antenna through the motorshaft tachometer.

SECTION 4
COMPARISON OF TEST AND ANALYTICAL RESULTS

4.1 FIELD TESTS

Sinusoidal steady-state frequency response tests were performed to determine the system frequency response to drive system excitation. In the horizon orientation, the response to azimuth excitation was measured. In the zenith orientation, response to both azimuth and declination excitation was measured. The antenna was excited by driving the servo valve with a HP202A function generator over the frequency range from 0.1 to 25 cps. A pressure transducer was installed on the azimuth drive system's hydraulic motors to monitor differential pressure proportional to driving torque. The torque amplitude was maintained at a constant level in the azimuth response tests. Thus, it was possible to determine acceleration/torque frequency response functions at points where acceleration (or velocity) was monitored. Clusters of three mutually perpendicular accelerometers were mounted on the antenna at both points where the reflector attaches to the reflector arms, making possible the measurement of elastic and rigid body motions of the reflector and permitting observation of coupling of orthogonal vibration modes.

Accelerometers were also mounted to measure two horizontal components of the motion of the steel tower at the azimuth bearing in order to determine the elastic motion of the tower. A three-axis accelerometer package was mounted on top of the concrete tower to determine elastic motion of the tower and the effect of foundation motion. Typical accelerometer installations are shown in Figs. 4-1, 4-2, and 4-3. The drive shaft velocities were measured with drive shaft tachometers to determine locked rotor resonances. Transient tests were performed in which the antenna was set into motion and the exciting force suddenly removed and the resulting free oscillation recorded. Resonant frequencies measured in these transient tests can be compared with resonant frequencies observed in sinudoidal frequency

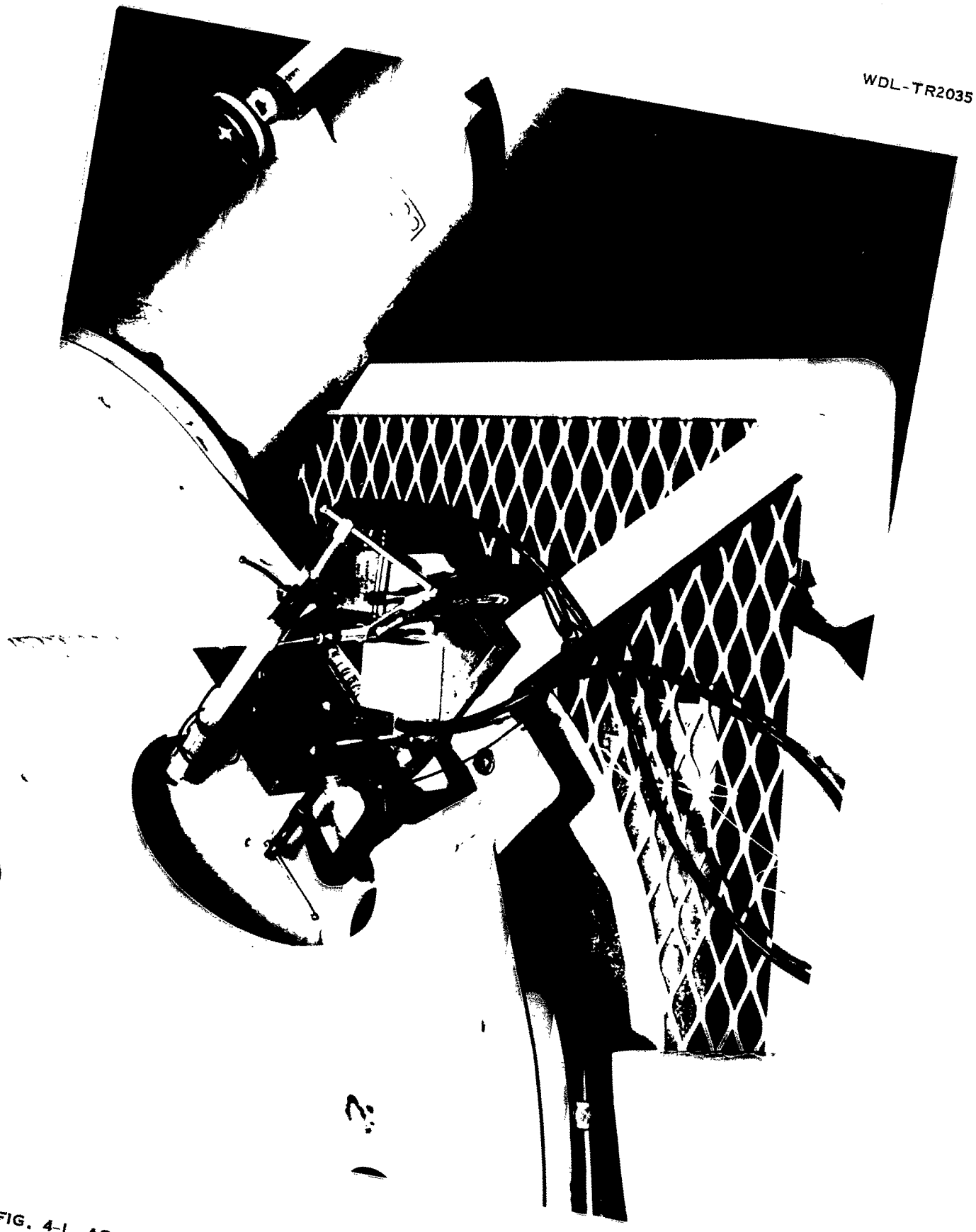

FIG. 4-1 ACCELEROMETER PACKAGE INSTALLATION AT THE FEED

FIG. 4-2 ACCELEROMETER INSTALLATION ON THE STEEL TOWER

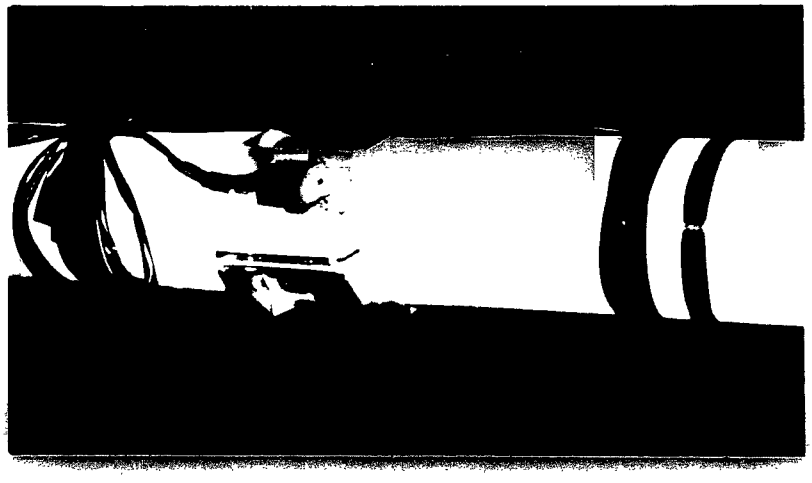

FIG. 4-3 ACCELEROMETER INSTALLATION ON A FEED SUPPORT LEG

response tests. In the above frequency response tests, all feedback loops were opened in order to isolate the dynamics of the structure from the dynamics of the feedback control system.

The frequency response data are presented as conventional Bode amplitude ratio diagrams in which the output-input amplitude ratio expressed in db was plotted as a function of the logarithm of frequency. The amplitudes used in the calculation of these amplitude ratios were determined by visually estimating from the strip chart records, the magnitudes of the fundamental components of the (sometimes non-sinusoidal) recorded waveforms. The occurrence of complex waveforms indicates the presence of non-linearities in the system and use of this "harmonic analysis" should yield the characteristics of the small amplitude, linear approximation to the system, which is useful in predicting response to arbitrary forcing functions. In general, no attempt was made to record absolute amplitudes, and curves given, therefore, show only the relative response at different frequencies.

In the tests in which the azimuth axis was driven, the motor torque (proportional to pressure) is considered to be the input. Since both acceleration and velocity were measured and because it is most meaningful to compare directly analagous parameters*, it was necessary (in the data reduction) to make use of the fact that if

$$x(t) = X \sin 2\pi ft, \qquad f = \text{frequency}$$

then

$$\dot{x}(t) = 2\pi f X \cos 2\pi ft$$

$$\ddot{x}(t) = (2\pi f)^2 X (-\sin 2\pi ft)$$

*Acceleration and torque, linear displacement and angular displacement

That is, velocity amplitudes can be obtained by multiplying displacement amplitude by the circular frequency, $2\pi f$ and acceleration amplitude can be obtained by multiplying velocity amplitude by $2\pi f$.

Two types of resonances are observed in these tests. The first type, known as locked-rotor resonances, are observed at frequencies which are natural frequencies of the antenna structure with the motor shaft brakes locked. At these frequencies, relative minima are observed on the motorshaft acceleration/torque frequency response functions. Knowledge of the frequencies at which these resonances occur is important in control system design. The second type of structural system resonances appear at frequencies at which relative maxima are observed on antenna acceleration/torque frequency response functions. Both types of resonances appear at frequencies which are peaks on antenna displacement/motor shaft rotation frequency response function. Locked-rotor resonances were observed in the azimuth vibration tests in this orientation at 2.3 cps, 5.5 cps, 10 cps, and 12 cps (see Fig. 4-4). The system resonant frequencies observed are listed below with brief descriptions of the phenomena observed at these frequencies.

3.2 - 5.5 cps. In this range of frequencies, peaks were observed in the response curves for all points sensitive to azimuth excitation. Some non-directly excited motion (such as the rotation of the reflector about its own axis) was also observed. In particular, a sharp peak in the pedestal's lateral motion response to declination excitation occurred at about 3.5 cps. There were apparently several modes of motion in this range in which lateral motion of the tower and torsion of the reflector about its own axis were coupled in different ways.

8.0 cps. A peak occurred at this frequency on the response of the reflector about its own axis, and an apparent flowering of the reflector was observed. Since this resonance was not generally reflected in the motions of the antenna, it probably is the fundamental resonant frequency of the reflector structure.

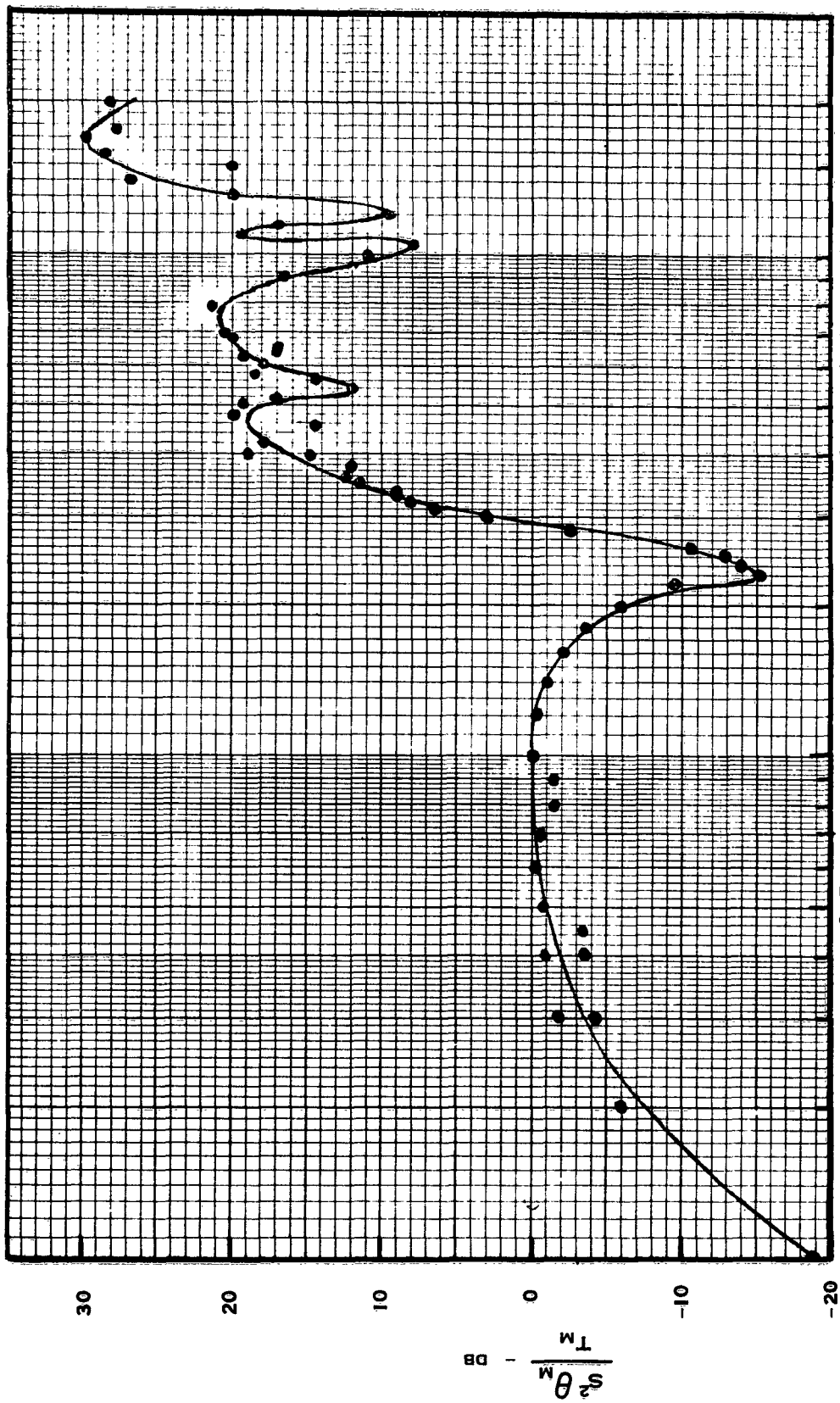

Fig. 4-4 Motorshaft Acceleration/Azimuth Motor Torque Frequency Response - Horizon Orientation

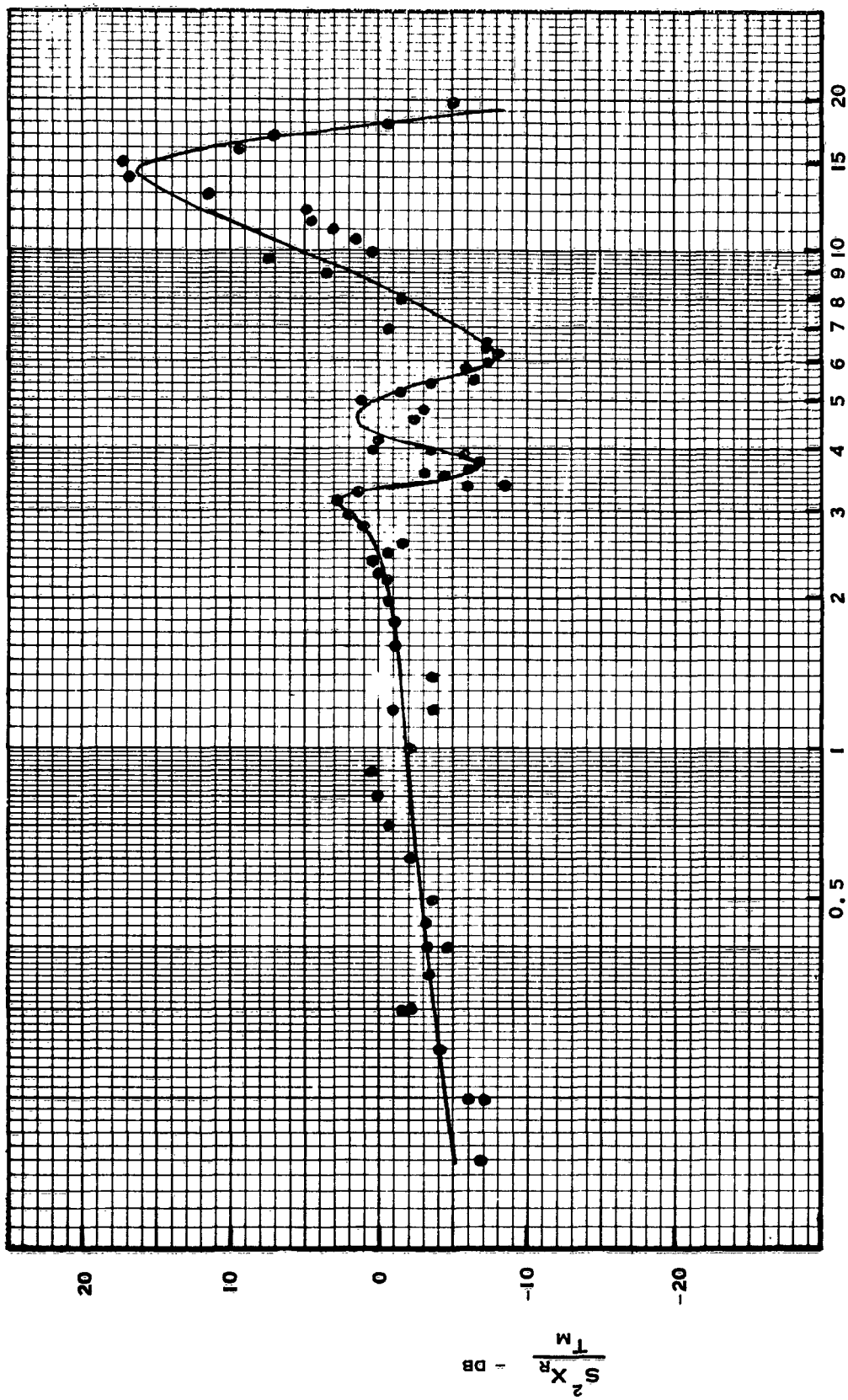

Fig. 4-5 Reflector Transverse Acceleration Azimuth Motor Torque Frequency Response - Horizon Orientation

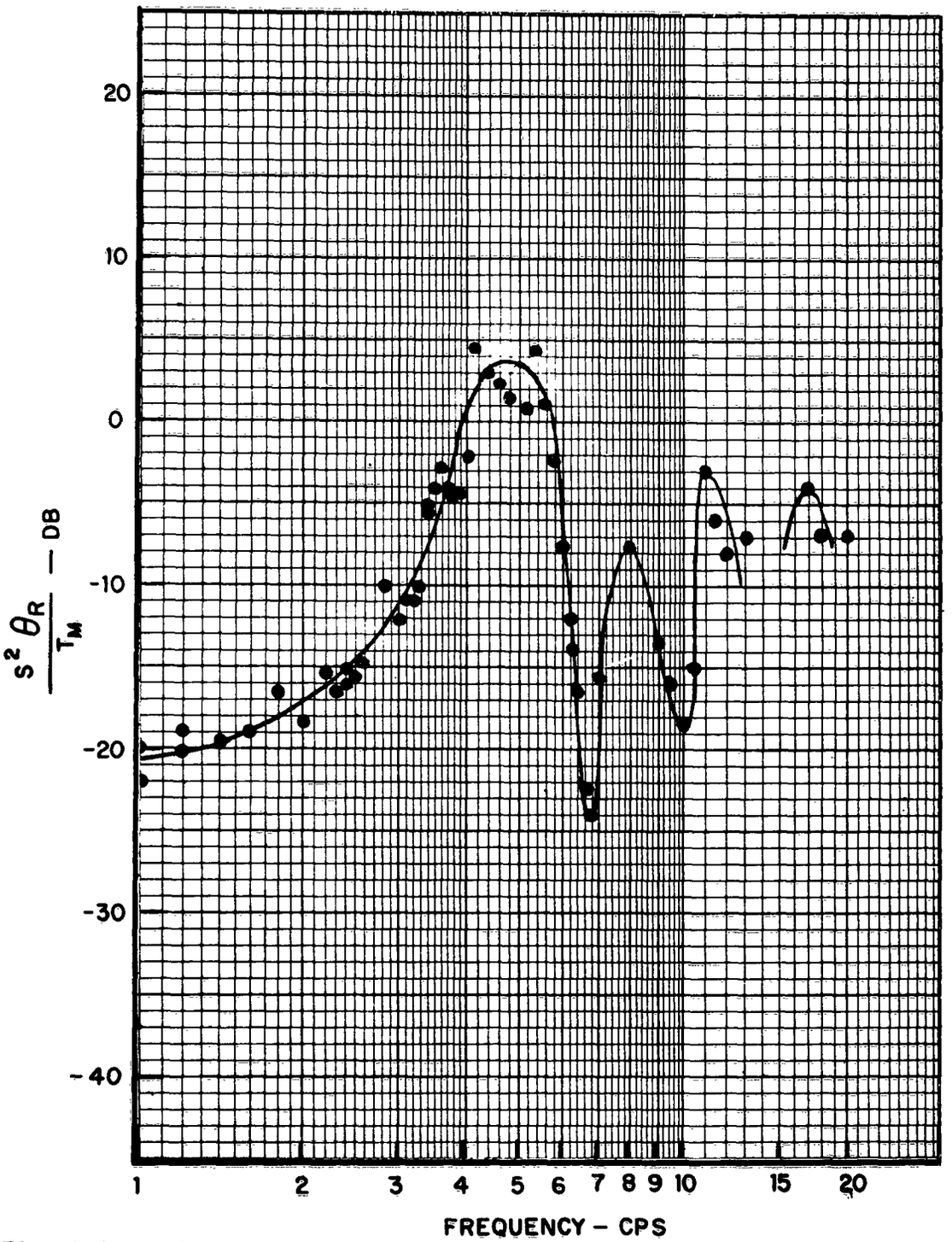

Fig. 4-6 Reflector Rotational Acceleration/Azimuth Motor Torque Frequency Response - Horizon Orientation

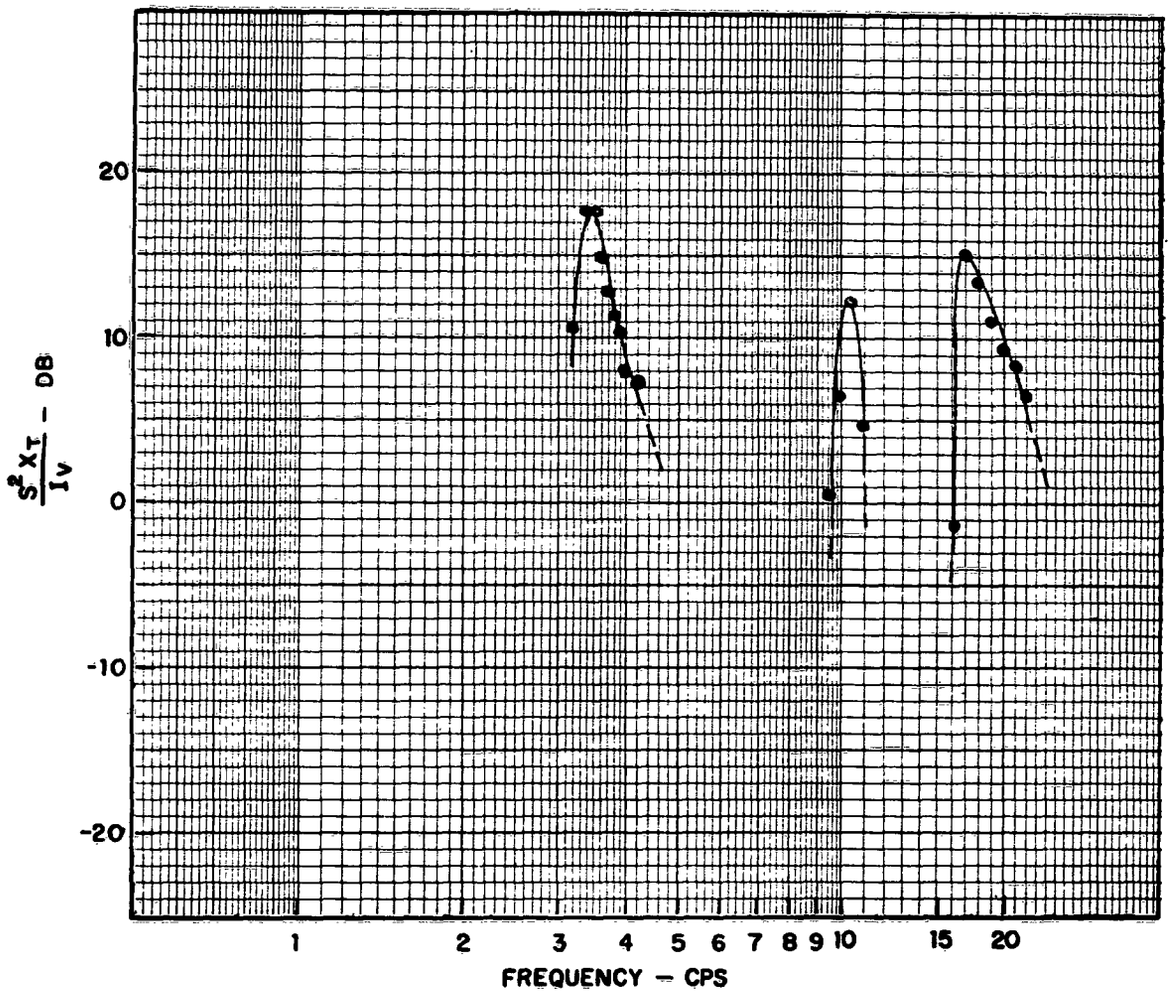

Fig. 4-7 Steel Tower Radial Acceleration/Declination Servo Valve Current Frequency Response - Zenith Orientation

11 cps. Peaks occurred on most response curves, including lateral pedestal motion.

16 cps. Peaks occurred on response curves for all points sensitive to azimuth excitation, including lateral pedestal motion.

Figures 4-5 through 4-7 illustrate experimental amplitude frequency response functions for lateral reflector translation; reflector rotation about its own axis; lateral motion of the pedestal about its own axis; and motor shaft rotation.

4.2 COMPARISON OF ANALYTICAL AND TEST RESULTS

4.2.1 System Resonant Frequencies

The denominator of the transfer functions discussed in Section 3 indicates system resonant frequencies of 3.5, 4.1, 5.0, 9.9 and 16.1 cps.

Examination of mode shapes corresponding to these frequencies show that, at 3.5 and 4.1 cps, the tower is experiencing unidirectional bending with amplitude increasing with height above ground and that the rotation of the reflector about its own axis is out of phase and in phase respectively with the rotation at the top of the tower. Analysis of a simplified model, in which only lateral motion of the tower was considered, and in which all of the moving antenna mass was concentrated at the top of the tower, yielded a lowest natural frequency of 3.8 cps. In the field tests, the amplitude response functions of sensitive points all exhibited some peaking in the 3.2 to 5.3-cps range and the observed modes appeared to involve various combinations of tower bending and reflector rotation. In particular, accelerometers mounted to measure lateral tower motions exhibited peaks at about 3.5 cps in both azimuth and declination excitation.

The third calculated system resonant frequency, 5.0 cps, is attributable to vibration of the feed support system as an almost isolated component. It has been found both experimentally and analytically that, while the feed support system is excited when the antenna is driven at the feed support resonant frequency, these resonances are only slightly coupled to the major structure and do not appear as significant peaks in experimental frequency response functions for hard points behind the reflector. In analysis, this phenomenon manifests itself in the appearance (in transfer functions for points behind the reflector) of zeros very close in frequency to the system resonant frequency corresponding to feed support resonance.

Examination of the mode shape corresponding to the 9.9-cps system resonant frequency again indicates a complex combination of lateral tower bending and reflector rotation. The second mode of vibration of the simplified tower bending model is 8.4 cps. Peaks are observed at sensitive points in the structure at about 11 cps, and again a sharp peak in the response of the tower lateral motion.

The last calculated system resonant frequency of 16.1 cps appears as a significant resonance in all the calculated transfer functions, and in all of the measured frequency response functions significant peaks occur in the 14 to 17-cps range. The response functions for the gross motion of the reflector are more or less "flat" until the appearance of the 15-cps frequency. The frequency interval between the lowest locked-rotor frequency (2.3 cps) and the first significant system resonant frequency (15 cps) is seldom as great as it is in this mode of excitation on this antenna.

A system resonant frequency was observed in the field at about 8 cps. This resonance was apparently the lowest natural frequency of the reflector structure because, (1) it only appeared as a peak in the reflector rotation frequency response, (2) no transient oscillation could be excited at this frequency, and (3) flowering motions of the

reflector were visually observed at this frequency. In the analysis, the reflector was considered to be a rigid body, thus precluding the appearance of reflector resonances in the analytical results. Consideration of reflector structure dynamics will be made in further analysis of the IOS antenna.

4.2.2 Locked Rotor Frequencies

The zeros of the motor shaft frequency response function indicate locked-rotor resonant frequencies of 2.7, 3.8, 5.0, 6.1 and 12.3 cps. The first of these is comparable to the lowest observed dip in the tachometer frequency response of 2.3 cps and corresponds to a natural mode of the system with the brakes locked in which the entire antenna is rotating about the azimuth axis. The second, 3.8 cps, is included in the complex of modes involving lateral tower bending and reflector rotation which are reflected in the measured tachometer frequency response as a general rise in the 3.5 to 4.5 cps range. The 5.0 cps frequency is due to the feed support system resonance, and, as discussed above, is not significantly felt as far back as the motor drive shaft. The next at 6.1 cps, corresponds to the dip in the measured response curve at about 5.5 cps. The final calculated locked-rotor frequency at 12.3 cps is seen experimentally as the dip preceding the 17-cps peak. In the above discussion of system resonant frequencies it was pointed out that, at 8 cps, a resonant frequency was observed that was not calculated and (in the case of the motor shaft frequency response) both a peak and a dip are observed in this general frequency range. These did not appear in the calculated transfer function because the reflector flexibility was not considered in the analysis.

SECTION 5
SPECIAL ANALYSES

5.1 INTRODUCTION

Several approaches were used to determine areas in which the structure is disproportionately flexible, because if such areas exist it should be possible to raise the significant natural frequency by stiffening these components. One attack on this problem involves simple comparison of compliances of various components. Another investigation involves performing dynamic analyses of various components of the antenna structure both to determine what effect they have on the overall structure and to determine how variations in the structural configuration affect the significant resonances of the overall structure. The results of these investigations are outlined below.

5.2 TOWER

A comparison of the torsional compliances of the elastic elements between the lumps in the tower model reveal that the equivalent compliance of the azimuth gear drive system is an order of magnitude greater than the compliance of any other individual element in this chain. A simplified model in which only rotations of the components about the azimuth axis were considered was analyzed. In this model, all of the mass of the moving structure was concentrated in a single lump at the top, and the torsional compliance between the gimbal and the declination drive housing was included. The lowest natural frequency (corresponding to a locked-rotor frequency) for this model was 5.5 cps. When the compliance of the transverse drive system was added between the gimbal and the moving structure beyond the gimbal, this frequency decreased to 4.5 cps. Inspection of the mode shape for the first model shows that, as is expected, the signicant increases in modal amplitudes occur across the azimuth bearing and between the declination drive housing and the moving structure, since these are the locations of the over-compliant components. In this model, these amplitude increments are about the

same because the azimuth drive system compliance (230×10^{-12} rad/in lb) is comparable to the compliance between gimbal and declination drive housing (164×10^{-12}). The latter compliance is primarily due to the radial flexibility of the declination axis bearings. In the second model, the increase in modal amplitude from declination drive housing to gimbal was about twice that across the azimuth bearing.

Since both of the preceding calculated frequencies are high compared to the calculated locked-rotor frequency for the over-all system (2.7 cps), it is evident that the overly-compliant components considered (azimuth and transverse drive systems and declination axis bearings) are not the sole cause of the low locked-rotor frequency observed in this orientation.

5.3 MOVING ANTENNA STRUCTURE

A dynamic analysis of the moving structure beyond the gimbal (shown in Fig. 2-2) was made to determine the natural frequency of that portion of the structure under conditions in which tower motion was constrained to isolate its contribution to the over-all locked-rotor frequency. In this analysis, the gimbal was assumed to be grounded. With this constraint, the only flexibilities in the system are those of the transverse drive system and bearings, and the reflector-counterweight, reflector ring assembly. The lowest resonant frequency of this structure was 3.0 cps, which is only slightly higher than the 2.7 cps locked-rotor frequency, so it can be inferred that a major contribution of the observed low frequencies comes from this group of components.

Inspection of the mode shape showed that, because of its asymmetry (the drive system is on one of the arms only, and the other is free-wheeling at the transverse axis), there were considerably larger amplitudes on the ungeared reflector arm at both the reflector and the counterweight. The model was then modified in such a way that half of

the transverse drive system was inserted at the transverse axis on both arms, as if the transverse axis were driven with one gearbox on each of the arms. The first resonant frequency of this modified symmetric structure rose to 7.4 cps. It can thus be inferred that, if the transverse axis were driven symmetrically, the locked-rotor frequency might be considerably increased.

5.4 BACK-SHAFT FREQUENCY RESPONSE

To obtain another indication of the effect of the azimuth drive system compliance on the locked-rotor frequencies, the frequency response for the rotation of the azimuth gear was calculated. The zeros of this response function are equivalent to the natural frequencies of the structure grounded at the azimuth bearing, and thus are not affected by drive system compliance. The first zero of this transfer function appeared at 2.8 cps compared to the lowest locked-rotor frequency, which was 2.7 cps. It thus appears that the azimuth drive system compliance has an inconsequential effect on the over-all system performance.

In systems in which gearing flexibility is significant, bandwidth could be increased by using a feed-back tachometer mounted on the pinion rather than on the motor shaft, but this change apparently would effect an insignificant improvement on the FGS system.

DISTRIBUTION LIST

Address	No. of Copies
Commander Space Systems Division Air Force Systems Command United States Air Force Air Force Unit Post Office Los Angeles, California Attn: Technical Data Center	10
USAF Contract Support Detachment No. 3 Philco Corporation Western Development Laboratories Palo Alto, California	1
ASTIA Arlington Hall Sta. Arlington 12, Virginia	10
Philco Corporation Western Development Laboratories Palo Alto, California	144 + 1 reproducible
Philco Corporation Plant 50 4700 Wissahickon Ave. Philadelphia 44, Pennsylvania Attn: D. Kinnier (Engineering)	1
Philco Corporation Plant 37 Union Meeting Road Blue Bell, Pennsylvania Attn: R. Murphy	1
Philco Corporation Computer Division 3900 Welsh Road Willow Grove, Pennsylvania Attn: Librarian	1
	168 + 1 reproducible